JOURNAL OF ENDOUROLOGY
Volume 29, Number 2, February 2015

Pp. 235–239
DOI: 10.1089/end.2014.0305

Influence of Saline on Temperature Profile of Laser Lithotripsy Activation

Wilson R. Molina, MD, Igor N. Silva, MD, Rodrigo Donalisio da Silva, MD, Diedra Gustafson, David Sehrt, and Fernando J. Kim, MD

Abstract

Purpose: We established an *ex vivo* model to evaluate the temperature profile of the ureter during laser lithotripsy, the influence of irrigation on temperature, and thermal spread during lithotripsy with the holmium:yttrium-aluminum-garnet (Ho:YAG) laser.

Materials and Methods: Two ex vivo models of *Ovis aries* urinary tract and human calcium oxalate calculi were used. The Open Ureteral Model was opened longitudinally to measure the thermal profile of the urothelium. On the Clinical Model, anterograde ureteroscopy was performed in an intact urinary system. Temperatures were measured on the external portion of the ureter and the urothelium during lithotripsy and intentional perforation. The lithotripsy group (n = 20) was divided into irrigated (n = 10) and nonirrigated (n = 10), which were compared for thermal spread length and values during laser activation. The intentional perforation group (n = 10) was evaluated under saline flow. The Ho:YAG laser with a 365 μm laser fiber and power at 10W was used (1J/Pulse at 10 Hz). Infrared Fluke Ti55 Thermal Imager was used for evaluation. Maximum temperature values were recorded and compared.

Results: On the Clinical Model, the external ureteral wall obtained a temperature of 37.4°C ± 2.5° and 49.5°C ± 2.3° ($P = 0.003$) and in the Open Ureteral Model, 49.7°C and 112.4°C with and without irrigation, respectively ($P < 0.05$). The thermal spread along the external ureter wall was not statically significant with or without irrigation ($P = 0.065$). During intentional perforation, differences in temperatures were found between groups (opened with and without irrigation): 81.8° ± 8.8° and 145.0° ± 15.0°, respectively ($P < 0.005$).

Conclusion: There is an increase in the external ureteral temperature during laser activation, but ureteral thermal values decreased when saline flow was applied. Ureter thermal spread showed no difference between irrigated and nonirrigated subgroups. This is the first laser lithotripsy thermography study establishing the framework to evaluate the temperature profile in the future.

Introduction

The holmium:yttrium-aluminum-garnet (Ho:YAG) laser has become the standard tool for intracorporeal management of stone disease because it has been shown to be effective in fragmenting all urinary calculi, independent of stone compositions.[1–3] Stone fragmentation phenomena are well understood, but there is currently a lack of information regarding the energy spread during this exogenous process. Iatrogenic damage to soft tissues can be caused by various forces related to devices such as thermal and mechanical interactions.[4,5] Complications entailed by ureteroscopy such as ureteral injury and strictures can be caused by displaced acoustic and photonic energy. Another potential cause of injury, however, can be direct thermal injury of the ureter. Different ureteroscopy techniques, irrigation devices, stone burden, laser activation time, and operative time can increase the exposure to these potential risks for laser lithotripsy related postoperative complications. We aimed to establish an *ex vivo* model to evaluate the temperature profile of the ureter during laser lithotripsy. In addition, we investigated the influence of irrigation on ureteral temperatures and on thermal spread along the ureteral wall.

Materials and Methods

The temperature profile of laser lithotripsy was evaluated with two *ex vivo* models of *Ovis aries* (sheep) urinary tract. On the Open Ureteral Model, the ureter was opened longitudinally to directly measure the thermal profile of the urothelium. The Clinical Model anterograde ureteroscopy was performed in an intact urinary system to replicate the clinical

Division of Urology, Department of Surgery, Denver Health Medical Center, University of Colorado, School of Medicine, Denver, Colorado.

environment (Fig. 1). In each model, the laser lithotripsy procedure (n = 20) was performed, and temperatures were collected. Thermocouples were used to calibrate the camera. A control test was performed measuring the temperature of the ureter tissue at room temperature of 23.9°C and also after tissue immersion in warm water at 50°C. Temperature was obtained simultaneously with the thermocouples and the camera, and the same values were achieved. Intentional perforation procedures (n = 10) were performed only on the Open Model to attempt to collect the temperature of the urothelium at the moment of the perforation.

During laser lithotripsy, the calculi were placed in the ureter, the laser fiber was brought into contact with the stone, the laser was activated, and the ureteral temperature was measured. During intentional perforation, the laser fiber was brought into contact with the urothelium and activated. A Ho:YAG laser (Dornier Medilas,™ Kennesaw, GA) with a 365 μm silica laser fiber (Gyrus ACMI,™ Southborough, MA) at a power of 10W (1J/Pulse at 10 Hz) was activated for 3 seconds. Human samples of calcium oxalate monohydrate stones ranging from 5 to 7 mm were fragmented during lithotripsy measurements. An infrared Fluke Ti55® Thermal Imager (Fluke® Corporation, Everett, WA) camera was used for the thermal evaluation. Temperatures were obtained with FLIR® SmartView Imaging Software. The maximum ureteral temperature achieved during laser activation was recorded.

The Open Ureteral Model permitted direct measurements of the urothelium temperature during perforation and laser lithotripsy (Fig. 1A). The *Ovis* ureter was dissected sharply longitudinally to expose the urothelium. In lithotripsy trials, a stone was placed in the ureter, and the laser was brought in contact with the stone. For intentional perforation measurements, the fiber was held at approximately 60 degrees to the urothelium and activated.

Laser lithotripsy in the Clinical Model was performed to replicate the clinical scenario (Fig. 1B). This model included an intact upper urinary tract system (kidney and ureter), a rigid ureteroscope, and saline irrigation with a pumping system (SAP™ - Single Action Pumping System, Boston Scientific,™ Natick, MA). Because of the small caliber of the distal ureter, antegrade access was obtained. The anterior renal parenchyma and collecting system were sharply dissected to obtain access to the renal pelvis. A small incision was made at the renal pelvis close to the ureteropelvic junction and a guidewire was inserted into the ureter followed by ureteral dilation up to 7F. An Olympus™ 7F semirigid ureteroscope with a stone inside a basket was inserted, and the stone was placed into the ureter. The basket was removed, and the laser fiber was inserted through the ureteroscope. Laser lithotripsy was performed with the Ho:YAG laser with a 365 μm silica laser fiber at a power of 10W (1J/Pulse at 10 Hz) and was activated for 3 seconds. Thermographic measurements were collected on the outer surface of the ureter.

The effect of saline irrigation on ureteral temperatures during laser activation was further evaluated. In each model, measurements were recorded with and without saline irrigation. In the Open Model, a saline bag was hung 3 feet above the *ex vivo* model using a tube set (Continu-Flo Solution Set with Duo-Vent Spike,™ Baxter Healthcare Corporation, Deerfield, IL) to apply constant irrigation with a mean flow rate of 8 mL/s. In the Clinical Model, we used the open irrigation system in conjuncture with a pumping system (SAP™). Irrigation was applied for visualization purposes to identify the calculus. Once the laser was in contact with the stone, irrigation was either continued or terminated for 30 seconds before laser activation.

In addition to maximum temperature, the distance of the thermal spread was also measured during laser activations. The length of thermal spread was recorded when the temperature elevated >5°C from room temperature. The thermographic images were imported into ImageJ (National Institute of Health, Bethesda, MD) and filtered to identify elevated temperatures. The maximum length of the heated segment was recorded.[6]

Data are presented as average ± standard error. The effect of irrigation was compared using Student *t* tests in The R Project version 2.11 (the R Foundation for Statistical Computing, Vienna, Austria). A *P* value ≤0.05 was considered statistically significant.

Results

This thermography study found a significant increase in the urothelium and external ureteral wall temperatures during the

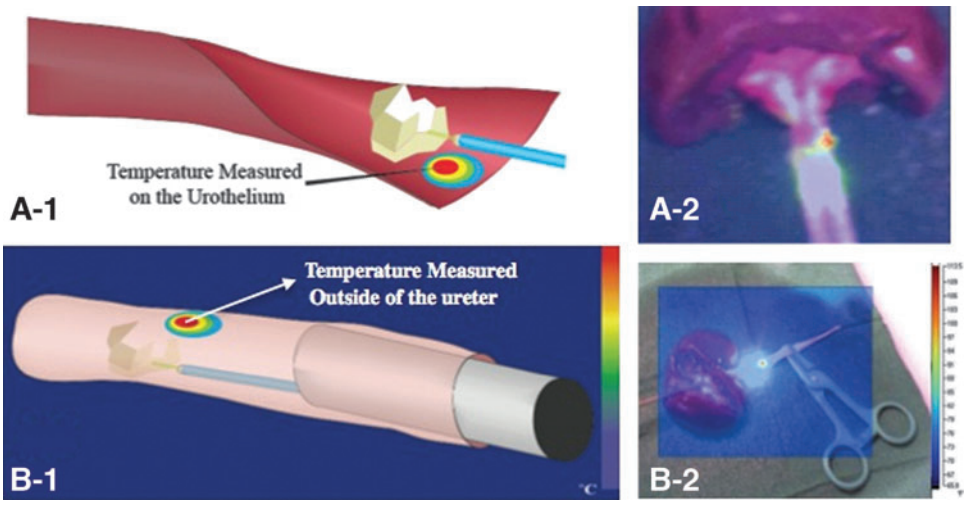

FIG. 1. The two *ex-vivo* models: **(A-1)** Open Ureter, **(A-2)** Open Ureter model temperature measurement; **(B-1)** Clinical Model **(B-2)** Clinical Model temperature measurement.

Table 1. Lithotripsy Temperature Profile and Thermal Spread

	Lithotripsy		
	Irrigation (°C)	*Nonirrigation (°C)*	P *value*
Intact Ureteral Model	37.4 ± 2.5	49.5 ± 2.3	0.003
Open Ureteral Model	49.7 ± 6.7	112.4 ± 24.2	0.048

Ho:YAG laser activation. In the Clinical Model, temperatures obtained were 37.4°C and 49.5°C with and without irrigation, respectively, and were significantly different ($P < 0.05$). In the Open Ureteral Model, there was also a significant increase in the temperature without irrigation (112.4°C) when compared with an irrigated trial (49.7°C) ($P < 0.05$). (Table 1) When evaluating the thermal spread length along the external ureter wall during lithotripsy, no significant differences were evident whether or not saline flow was applied. The thermal spread along the external ureter wall was 0.9 ± 0.1 cm with irrigation and 1.1 ± 0.1 cm without ($P = 0.065$). (Table 2)

During intentional perforation, significant differences in temperatures were found between the Open Ureteral Model with and without irrigation, respectively, at 81.8°C ± 8.8°C and 145.0°C ± 15.0°C ($P < 0.005$) (Table 3).

Table 3. Temperature Profile During Intentional Perforation of the Ureter

	Temperature during ureter perforation (°C)		
	Irrigation	*Nonirrigation*	P *value*
Open Ureteral Model	81.8 ± 8.8	145.0 ± 15.0	0.003

Discussion

The Ho:YAG laser is widely used in the surgical management of urinary lithiasis. Since its introduction in the 1990s, the Ho:YAG laser has become the most common type of laser used for the treatment of patients with urinary stones.[5] Laser lithotripsy significantly improved results of ureteroscopy by improving stone-free outcomes when compared with pneumatic lithotripsy.[6,7]

Several types of lasers are available for clinical purposes. In general, these lasers can be categorized into groups according to their pulse duration time (T*p*): Nanosecond lasers (T*p* < 1000 nsec) [Q-switched ND: YAG, Q-switched alexandrite, Q-switched ruby, XeCl excimer, short-pulsed lasers (1 μsec < T*p* < 10 μsec) Flashlamp-Pumped Pulsed-Dye, Flashlamp-Pumped Ti:Sapphire, Q-switched KTP], long-pulsed lasers (10 μsec < T*p* < 1000 μsec) [Ho:YAG, Er:Cr:YSGG, ND:YAG], and continuous-wave lasers (continuous pulse duration - T*p*) [CW-CO_2, CW-Nd: YAG].[8]

Nanosecond and short-pulsed laser lithotripters fragment stones through acoustic shockwaves.[8] The emission process from the acoustic shockwaves is closely related to the short pulse duration profile of these lasers. These short pulse-width lasers rapidly generate and accumulate energy in water (stress confinement phenomena), inducing a rapid formation and expansion of a spherical plasma cavitation bubble at the laser fiber tip. This bubble expands symmetrically, then collapses violently, releasing a strong photoacoustic shockwave in a process known as laser-induced shockwave lithotripsy.[8,9] The collapse of this bubble can be hindered if the laser energy is continuously emitted, as in a long pulse.[6]

Table 2. Lateral Thermal Spread of Laser Lithotripsy

	Lateral thermal spread		
Heated length (cm)	*Irrigation*	*Nonirrigation*	*P value*
Intact Ureteral Model	0.9 ± 0.1	1.1 ± 0.1	0.065

Lasers differ significantly in wavelength and pulse width. The Ho:YAG laser, with a wavelength of 2120 nm, is close to the absorption peak of water (1940 nm), and it is usually used with a pulse duration of 500 μs, longer than that of the previous lasers.[6,7] The Ho:YAG vapor bubble does not result in significant cavitation shockwaves, and lithotripsy occurs long before the vapor bubble has collapsed, suggesting that acoustic shockwave emission is not the primary mechanism for stone fragmentation.[10,11] The primary mechanism of action for long-pulsed lasers such as the Ho:YAG laser, is thought to be the photothermal effect.[11] This mechanism involves the direct absorption of photonic energy by the stone, inducing a melting and fragmentation process.[11,12] Ho:YAG energy absorption by the stone increases the stone temperature until a critical thermal threshold is achieved. At this thermal threshold, the stone may chemically decompose and may also cause the interstitial water to undergo explosive vaporization.[11,13] The volume of the irradiated area is detached from the stone, yielding a crater.[14] Melting point thresholds for magnesium ammonium phosphate dihydrate, calcium hydrogen phosphate dihydrate, calcium oxalate monohydrate, and cystine stones are 100°C, 109°C, 206°C, and 264°C, respectively.[15]

The Ho:YAG laser-stone photothermal interaction occurs under a thermal confinement process. Photothermal removal of the calculus through melting, carbonization, or chemical decomposition is confined to the region of light absorption.[16,17] The speed at which heat leaves the light absorption site (thermal diffusion time) plays an important role in clinical lithotripsy application regarding safety of the procedure. When the laser pulse duration (T*p*) is much shorter than the thermal diffusion time, there is little heat conduction outside the stone-irradiated site during the laser pulse. This results in focal stone destruction of the irradiated volume before the heat is conducted to the surrounding tissues. When the pulse duration is longer than the thermal diffusion time, the heat energy travels beyond the region of direct laser absorption site during the laser pulse, causing damage on surrounding tissues such as coagulation and carbonization.[16]

The stone and ureteral environment can affect the efficiency of stone decomposition. Stone fragmentation analysis demonstrated greater stone mass losses after lithotripsy was

performed with dry stones in air when compared with wet stones in air, which was greater than for stones in water. In addition, lithotripsy led to greater stone mass losses when stones started at 20°C rather than −80°C.[11] Pierre and Preminger[18] suggest that lithotripsy is more efficient for dry stones and that the efficiency increases as the initial stone temperature increases. Evidence also shows that the efficiency of Ho:YAG laser lithotripsy varies with greater energy exposure to the stone surface, implying that the stone absorbs laser energy.[14] These findings demonstrate the importance of the direct absorption of the laser energy by the stone composition.

In this scenario, a phenomenon called the ''Moses Effect'' further enhances the Ho:YAG laser fragmentation process. The Moses Effect is the expansion of a vapor cavity that eventually bursts and distributes the acoustic energy and pressure waves throughout the medium. Although acoustic energy released from the bubbles is not the primary mechanism for damaging the stone, these bubbles greatly improve the transmission of photonic energy to the stone. The coefficients of absorption (μ_a) for the Ho:YAG laser in water (l) and vapor (g) are $25\,cm^{-1}$ and $0.015\,cm^{-1}$, respectively.[16,18] This physical property demonstrates that the initial beam of the Ho:YAG laser pulse duration vaporizes a channel through which the laser energy may transmit efficiently to the stone.[11,19]

Several aspects of heat action on biologic tissues have already been examined in numerous preclinical and clinical studies. The *in vitro* and animal hyperthermic experiments demonstrated a direct cellular destruction effect at temperatures ranging from 41°C to 47°C. This cytotoxic effect was shown to be exponentially enhanced at temperatures above 43°C (''breakpoint'').[20–22] These thermal cytotoxic effects, however, are not exclusively related to the absolute peak temperatures achieved during a procedure. Indeed, the relationship between time and temperature for thermal death was demonstrated *in vitro* and *in vivo*, and thermal damage was shown to increase as the time at an elevated temperature increases.[23,24] In addition, a unit of thermal dose was determined for equating time-temperature relationships for an isoeffect (same amount of cell killing) to an equivalent time duration at a reference temperature of 43°C, represented on the formula for equivalents minutes at 43°C ($t_{43} = t \,.\, R^{(43-T)}$, where t = time, T = Temperature, $R = 0.5$ for T equal to or more than 43°C, and $R = 0.25$ for T less than 43°C).[5] Summarizing, it means that at temperatures above 43°C, the time needed to produce an isoeffect must be decreased by a factor of 2 when temperature is elevated 1°C.[25] Consequently, a 30-minute treatment at 44°C is equivalent to 60 minutes at 43°C, which is also equivalent to 15 minutes at 45°C for the same effect.

Our experiment showed an increase in the external ureteral temperature during the Ho:YAG laser activation. When saline irrigation flow was applied, a remarkable reduction on ureter thermal values during lithotripsy was achieved. We hypothesized that the photothermal effect of Ho:YAG laser could have been attenuated as a consequence of the continuous saline flow. The constant saline flow could have absorbed part of the Ho:YAG laser wavelength energy that should have been discharged directly to the stone surface, leading to lower ureter thermal measurements. Irrigation may have also produced a ''heat-sink'' as cooler water dissipated heat by cycling through the system. Another hypothesis is that the Moses Effect could have been partially affected by saline flow, hindering the vapor channel created by the laser beam. This process, in turn, could have reduced both the photonic energy transmittance to the stone surface and the efficiency of lithotripsy, leading to lower temperature measurements. The thermal spread length did not vary significantly during lithotripsy regardless of irrigation or nonirrigation status. Furthermore, intentional perforation of the ureter showed a significantly higher thermal profile than during lithotripsy, which emphasizes the safety concerns of performing lithotripsy without constant irrigation. Therefore, steady saline flow is encouraged to avoid ureteral thermal injury.

Limitations of this study are: Use of a nonhuman organ, use of an *ex-vivo* model, the use of one size of laser fiber, and the response time of the camera. Although the tissue used was not human, the experimental design accurately replicated the laser lithotripsy procedure. The *Ovis aries* urinary tract presented differences in the thickness of tissue and fat dispersion when compared with human ureters, and these differences could lead to inaccurate temperature measurements. The *ex-vivo* models are unable to be histologically evaluated to accurately demonstrate the extent of tissue necrosis and potential ureteral stricture. Further studies using a live model could address tissue necrosis and microvascular damage over time (thermal dose), and histopathological analysis should be collected. Another issue is that the *ex-vivo* model was not kept at the standard body temperature of 37°C, possibly affecting heat generation and dispersion. Ideally, the *ex-vivo* model should replicate conditions found in *in-vivo* models. We looked at temperature differences using one size (365 μm) of laser fiber and maximum values may vary with fiber size, but the difference with and without irrigation is expected to follow the same trends. Further studies varying laser fiber sizes are needed. The camera has a limitation within the refresh rate of 3 seconds, but the temperatures were recorded at the end of the time interval to ensure that we collected the highest temperature.

Conclusion

A notable increase in the external ureteral temperature has been observed during Ho:YAG activation. Another observation was that ureteral lithotripsy thermal values showed a remarkable reduction when constant saline flow was applied. Ureter thermal spread evaluation showed no statistical difference when irrigated and nonirrigated subgroups were compared. During intentional perforation of the ureter, thermal values were higher than during laser lithotripsy measurements. Irrigation not only improved endoscopic visualization during lithotripsy but also minimized tissue heating. Interruption of the saline flow could pose a risk for urothelial thermal injury. This is the first laser lithotripsy thermography study that establishes the framework to evaluate the temperature profile in the future.

Disclosure Statement

No competing financial interests exist.

References

1. Teichman JM, Vassar GJ, Bishoff JT, Bellman GC. Holmium:YAG lithotripsy yields smaller fragments than

lithoclast, pulsed dye laser or electrohydraulic lithotripsy. J Urol 1998;159:17–23.
2. Teichman JM, Rogenes VJ, McIver BD, Harris JM. Holmium:yttrium-aluminum-garnet cystolithotripsy of large bladder calculi. Urology 1997;50:44–48.
3. Razvi HA, Denstedt JD, Chun SS, Sales JL. Intracorporeal lithotripsy with the holmium:YAG laser. J Urol 1996;156: 912–914.
4. van de Berg NJ, van den Dobblesteen JJ, Jansen FW, et al. Energetic soft-tissue treatment technologies: An overview of procedural fundamentals and safety factors. Surg Endosc 2013;27:3085–3099.
5. Sapareto SA, Dewey WC. Thermal dose determination in cancer therapy. Int J Radiat Oncol Biol Phys 1984;10:787–800.
6. Khalil M. Management of impacted proximal ureteral stone: Extracorporeal shock wave lithotripsy versus ureteroscopy with holmium: YAG laser lithotripsy. Urol Ann 2013;5:88–92.
7. Molina WR, Marchini GS, Pompeo A, et al. Determinants of holmium:yttrium-aluminum-garnet laser time and energy during ureteroscopic laser lithotripsy. Urology 2014; 83:738–744.
8. Aboumarzouk OM, Somani BK, Monga M. Flexible ureteroscopy and holmium:YAG laser lithotripsy for stone disease in patients with bleeding diathesis: A systematic review of the literature. Int Braz J Urol 2012;38:298–306.
9. Atis G, Gurbuz C, Arikan O, et al. Uteroscopic management with laser lithotripsy of renal pelvic stones. J Endourol 2012;26:983–987.
10. Cornu JN, Rouprêt M, Carpentier X, et al. Oncologic control obtained after exclusive flexible ureteroscopic management of upper urinary tract urothelial cell carcinoma. World J Urol 2010;28:151–156.
11. Chan KF, Pfefer TJ, Teichman JM, Welch AJ. A perspective on laser lithotripsy: The fragmentation processes. J Endourol 2001;15:257–273.
12. Sea J, Jonat LM, Chew BH, et al. Optimal power settings for Holmium:YAG lithotripsy. J Urol 2012;187:914–919.
13. Schafer SA, Durville FM, Jassemnejad B, et al. Mechanisms of biliary stone fragmentation using the Ho:YAG laser. IEEE Trans Biomed Eng 1994;41:276–283.
14. Finley DS, Petersen J, Abdelshehid C, et al. Effect of holmium:YAG laser pulse width on lithotripsy retropulsion in vitro. J Endourol 2005;19:1041–1044.
15. Vassar GJ, Teichman JM, Glickman RD. Holmium:YAG lithotripsy efficiency varies with energy density. J Urol 1998; 160:471–476.
16. Zhong P, Tong HL, Cocks FH, et al. Transient cavitation and acoustic emission produced by different laser lithotripters. J Endourol 1998;12:371–378.
17. Jensen ED, van Leeuwen TG, Motamedi M, et al. Temperature dependence of the absorption coefficient of water for midinfrared laser radiation. Lasers Surg Med 1994;14: 258–268.
18. Pierre S, Preminger GM. Holmium laser for stone management. World J Urol 2007;25:235–239.
19. Vassar GJ, Chan KF, Teichman JM, et al. Holmium:YAG lithotripsy: Photothermal mechanism. J Endourol 1999;13: 181–190.
20. Teichman JM, Vassar GJ, Glickman RD. Holmium:yttrium-aluminum-garnet lithotripsy efficiency varies with stone composition. Urology 1998;52:392–397.
21. Welch AJ, van Gemert MJ, eds. Optical-Thermal Response of Laser-Irradiated Tissue. New York: Plenum Press, 1995.
22. Urano M, Kuroda M, Nisimura Y, et al. For the clinical application of thermalchemotherapy given at mild temperatures. Int J Hyperthermia 1999;15:79–107.
23. Miller MW, Ziskin MC. Biological consequences of hyperthermia. Ultrasound Med Biol 1989;15:707–722.
24. Dickson JA, Calderwood SK. Temperature range and selective sensitivity of tumors to hyperthermia: A critical review. Ann N Y Acad Sci 1980;335:180–205.
25. Dewey WC. Interaction of heat with radiation and chemotherapy. Cancer Res. 1984;44(suppl 10):4714s–4720s.

Address correspondence to:
Wilson R. Molina, MD
Division of Urology, Department of Surgery
Denver Health Hospital Authority
777 Bannock Street
Denver, CO 80204

E-mail: Wilson.Molina@dhha.org

Abbreviations Used

Ho:YAG = holmium:yttrium-aluminum-garnet
T*p* = pulse duration